Dynamic behavior of humid granular avalanches: Optical measurements to characterize the precursor activity

Luc Oger ⬡,[*] Claude el Tannoury,[†] and Renaud Delannay ⬡[‡]
Univ. Rennes, CNRS, IPR (Institut de Physique de Rennes)-UMR 6251, F-35000 Rennes, France

Yves Le Gonidec ⬡[§]
Univ. Rennes, CNRS, Géosciences Rennes-UMR 6118, F-35000 Rennes, France

Irene Ippolito ⬡[‖] and Yanina Lucrecia Roht ⬡[¶]
Universidad de Buenos Aires, Facultad de Ingeniería, Grupo de Medios Porosos, Av. Paseo Colón 850, Buenos Aires, Argentina

Iñaki Gómez-Arriaran ⬡[**]
ENEDI, Department of Thermal Engineering, University of the Basque Country-UPV/EHU, Spain

Laboratory study of slope stability of granular media remains a challenge for modeling, understanding, and predicting natural hazards, such as avalanches and landslides, precursory signs of which are controlled by numerous physical parameters. The present work focuses on the impact of the humidity, in the range of 40–90%, on the stability of monodisperse dense packings of spherical beads. The beads are in a transparent box that is slowly and continuously tilted and allows simultaneous top and lateral optical measurements of global displacements of grains at the surface, defined as precursors. Humidity increases the cohesion between the grains. By performing successive avalanches that destabilize deeper granular layers, we assess the role of the exposure time to the high humidity rates in the diffusion process to reach the hygroscopic equilibrium inside the packing. We highlight an increase of the stability and first precursor angles, associated to a constant angle increment between two consecutive precursors, with a dependency with both the diameter (0.2, 0.5, and 0.75 mm) and the material (glass and polystyrene) of the grains.

I. INTRODUCTION

Organized displacements of granular materials are physical processes widely observed in a large range of industrial processes, such as concrete and ceramic preparations, transport of pharmaceutical products, agricultural grains, soils and powder metallurgy. In these cases, numerous grains are stored, pilled, or displaced. Similar processes may also be observed in many natural events such as flying ashes, debris flows and avalanches [1–3]. Better understanding the physical mechanisms that control such granular dynamics is challenging for numerous industrial and environmental topics, with first importance to prevent avalanches, for instance.

With that aim, laboratory experiments are usually performed with granular piles, which consist in dense packings of spherical grains under controlled conditions. A box containing the grains is continuously tilted to reach slowly the avalanche in a quasi-static regime of destabilization. When tilting the granular pile, the tangential component of the weight of the pile increases: this induces internal friction and leads the superficial layer of grains to a metastable state. When the tilt angle becomes greater than the maximum stability angle θ_A, the avalanche occurs. Before the avalanche, when the tilt angle is $\theta < \theta_A$, simultaneous displacements of the grains uniformly distributed at the surface of the pile without changing the inclination of its surface may be observed and define the so-called precursors. After the avalanche, the surface of the pile is rearranged to reach the angle of repose θ_R.

In wet conditions, the behavior of the slope stability may change because moisture increases the cohesion, i.e., the interaction forces that alter the strength of the contacts between the grains [4]. These behaviors are related to capillary interactions induced by liquid bridges which depend on the moisture content [5]. Some authors [6,7] have studied the relationship between cohesion and adhesion forces between grains in a pile when an isolated ring is created at the contact between two grains contacts, i.e., the external form is defined as a meniscus. These studies have also established that the maximum stability angle θ_A varies exponentially with the initial waiting time managed before the experiments. Unfortunately, they have performed experiments only up to 45% of relative humidity (RH), which is far from the range over which the influence on

————
[*]luc.oger@univ-rennes1.fr
[†]claude-el-tannoury@univ-rennes1.fr
[‡]renaud.delannay@univ-rennes1.fr
[§]yves.legonidec@univ-rennes1.fr
[‖]iippoli@fi.uba.ar
[¶]yroht@fi.uba.ar
[**]gomez.arriaran@ehu.eus

the stability and cohesion of the granular medium is expected to be very significant.

The present study focuses on the analysis of the impact of humidity on the precursor activity and is an extension of the previous experimental studies to the case of wet atmospheres: such high humidity, up to 100%, exist naturally very often in Argentina where our experiments took place. In Sec. II, we introduce both the description of precursors based on previous works on dry avalanches and the impact of humidity on the grain packing. In Sec. III, we describe the experimental method used to prepare the homogeneous packings of spheres in a wet atmosphere, the principles of the experiments and the optical measurements. In Sec. IV, we present the experimental results showing the importance of the diffusion of the humidity inside the pile of 500-μm glass beads, its consequence on the avalanche and precursor angles dependence with the height of the pile on one hand and the humidity rate on the other hand. In Sec. V, we highlight the effect of high humidity rates, size, and material of the grains on the precursor and avalanche behaviors.

II. PREVIOUS STUDIES ON DRY AVALANCHE PRECURSORS AND SEPARATE HUMIDITY EFFECTS

The discrete nature of granular materials makes their behavior very complex. At rest, a granular packing can sustain normal loads and shear stresses, such as a jammed structure [8]. When the packing is tilted, the shear stress may exceed a threshold and part of the pile starts to flow and the macroscopic behavior of the packing is related to geometry changes of the contact network and more specifically to the nature of the contacts which can be frictional, collisional, sliding, or cohesive [9]. For free surface flows, the critical shear stress is evidenced by the existence of the angle of maximum stability θ_A associated to internal friction properties [10]. When the tilt stops, the angle of the pile relaxes toward the angle of repose ($\theta_R < \theta_A$). Similar observations were made for granular flows in a rotating drum as a function of the rotation rate [11]. Generally, experiments are performed at a low rotating regime defined as the rolling or cascading regime controlled through the Froude number $\mathrm{Fr} = \omega^2 D/(2\,g)$ ($0.05 < \mathrm{Fr} < 0.4$), which corresponds to the ratio between the centrifugal acceleration defined by the angular speed ω and the system length D (drum diameter or plate dimension), to the gravitational acceleration g [12].

A. Context of dry avalanches

By the use of an optical camera and a digital imaging technique, Bretz *et al.* [13] were the first to reproduce and observe the destabilization of the pile, characterized by rearrangements of the grains located at the surface: they put in evidence that the rearrangement distribution follows a power law as a function of the bead diameter. They did not describe large events that occur between two avalanches but they have highlighted two kinds of events located before the avalanche: (i) small rearrangements that occur at low tilt angles with a power-law size distribution followed by (ii) the so-called precursors that appear quasi periodically when $\theta \gtrsim 15°$ with a non-power-law size distribution.

Nerone *et al.* [14,15] have shown that the size of the rearrangements increases with the tilt angle for freshly prepared piles filling a box and that quasiperiodical large events can be observed few degrees before the first maximum stability angle.

Aguirre *et al.* [16] concluded that the number of grain layers can influence the stability of a packing up to about ten layers, while it becomes independent of it for larger numbers of layers. This can be easily related to the well-known wall effect in granular packings [17].

By the use of acoustic methods, Zaitsev *et al.* [18] reported similar events in the bulk of the pile, interpreted as quasiperiodic transient reorganizations of the weak-contact subnetwork.

Kiesgen de Richter *et al.* [19] have studied the ageing effects and the influence of the initial preparation of the packing. They stated that the ageing stabilizes the packing and the activity of the packing was shown to depend strongly on the history of the system. Thus, information on that past history is crucial and is in some way stored in a specific texture of contact between grains.

Duranteau *et al.* [20] have demonstrated the strong correlations between optical and acoustical detections of precursors. They have shown that precursors are both of geometrical nature (at least at the surface) and of elastic nature in the bulk of the layer (at least down to a certain depth).

In complement, by developing a numerical approach, Staron *et al.* [21] investigated the evolution of the internal state of a 2D granular slope driven toward its stability limit and have related precursors of avalanches to the intermittent mobilization of friction forces between the grains along some long-range correlations of the structure. Amon *et al.* [22] have shown that it is possible to detect the precursors in the volume of the granular pile by an interferometry technique based on diffusive wave spectroscopy: Amon *et al.* [22] have observed an increase in the precursor intervals with humidity. In addition, they have founded that the appearance of the first precursor takes place at a smaller angle [22] for higher RH. They assumed that the rearrangements of grains occurring at high humidity imply a larger number of grains due to the cohesion of the medium leading. In complement, Amon *et al.* [23] have developed a simple 1D frictional model which can explain these precursor events and their quasiperiodicities. So all these processes of pile stability are controlled by several physical factors, including the size of the system (height [24], length [25], width [26–29]), the density or volume compaction of the packing [16,24,25,30,31] and the tilting regime [32–34].

But all these first experiments [14,16,24,35] and more recent studies [20,25,36,37] dedicated to the identification of the precursors have been essentially performed in a dry atmosphere, with a relative humidity up to about 50%.

B. Influence of the humidity

When humidity is taken into account, the structure of a granular medium is composed of three phases: the solid grains, the gas matrix, and the wetting liquid, the amount of which is quantified by the RH. The relative humidity is the relative vapor pressure P_v/P_{sat}, where P_v and P_{sat} are

the vapor and saturated pressures of water, respectively, at a given temperature. So RH depends on the temperature and the pressure of the system. Depending on RH, the pile can be characterized by different states [38]. In the pendular state, the pore space is filled by the gas phase and the liquid phase is discontinuous, located around the contacts between the grains; in the funicular state, the liquid phase is continuous and in the capillary state, the pore space is completely filled by the wetting liquid. The literature about the impact of RH on a pile stability remains very rare and the work by Gómez-Arriaran *et al.* [39] is a reference. In their study, the authors show that for glass beads of diameter 0.5, 1, and 2 mm and RH in the range 5–97%, the maximum stability angle θ_A and the repose angle θ_R are invariant in the pendular state and then increase with RH: For RH higher than 84%, θ_A can be as high as 90° for piles composed of small grains where cohesion forces are very strong [40]. Rumpf [41] proposed a model for determining the cohesion tension in a granular medium of identical spherical grains from the force of cohesion per liquid bridge. Crassous *et al.* [40] have shown the evolution of the adhesive force between two grains versus distance at a given humidity rate through atomic force setup measurements.

Other authors [42–44] noted that the depth of the avalanche plane and the angle of repose correlate with the moisture content up to a maximum saturation value, which depends on the grain size only. Fraysse *et al.* [45] have controlled RH by injecting water vapor inside a rotating drum containing the grains, and have quantified RH. They stated that θ_R slightly decreased and θ_A increased when moisture content increases.

In Mason *et al.* [46], a wedge of wet granular packing is tilting down to the horizontal and was used to determine the relationship between the angle of maximum stability θ_A and moisture, which is referred here to the volume fraction of liquid versus the total volume of the sample. Other authors [16,24] showed an increase of the maximum stability angle θ_A with RH and the number of layers for an inclining box filled with 2-mm-diameter glass beads.

One of the key questions of these methods is that the humidity is, maybe, not necessarily homogeneously distributed inside the pile: Facing this difficulty is not straightforward. Recent researches demonstrate the linear dependency between the angle of maximum stability and the time of exposition to ambient relative humidity before the avalanche [47]. Indeed, the rigorous control of RH and hygroscopic equilibrium time is necessary to avoid this inhomogeneity and to achieve a uniform distribution of the moisture content inside the granular medium at a given hygroscopic and cohesive state. The use of different heights of grains inside the box participates to the analysis of the humidity diffusion inside this porous media as we have used the range from the values of 3, 4, and 6 cm heights for the three high humidity values (RH = 75, 84, 94%, see below). Indeed, the percolation of the water vapor through the porous structure can only occur through the upper surface of the packing and depends strongly of the permeability of this porous structure which is quite small for 500-μm-diameter beads.

III. DESCRIPTION OF THE EXPERIMENTAL SETUP

To study the effect of humidity on the activity of both precursors and avalanches, we have designed a specific exper-

imental setup: the preparation of the pile, which is a dense packing of monodisperse spherical grains with a particular humidity, the experimental frame, which allows tilting the box containing the grains, and the optical measurements, composed of two cameras to capture the rearrangements of the superficial grains simultaneously from the top and lateral views of the pile.

A. Pile fabrication

In our experiments, we consider different piles composed of monodisperse spherical grains: glass beads with 0.20 mm $\pm$ 0.01 mm, 0.50 mm $\pm$ 0.18 mm, and 0.75 mm $\pm$ 0.18 mm diameters, and polystyrene grains with 0.14 mm $\pm$ 0.05 mm diameters. The grains are contained in a Plexiglas box, 6.5 cm in width, 11 cm in length, and 6 cm in height. The ambient temperature is maintained between 20 and 22°C for all our experiments.

The preparation of the pile is not a study parameter but requires a reproducible approach to focus the analysis on the effects of external parameters, in particular humidity. We have achieved this goal following the so-called "same history" of a pile fabrication [48]: (i) We place a grid with a square mesh of 12 mm (larger than the grain diameter) at the bottom of the box; (ii) we partially or fully fill the box with grains to prepare piles with different heights, from 2 to 6 cm; (iii) we shake horizontally the box to flatten the surface of the pile; (iv) we pull the grid out vertically to generate a homogeneous packing structure with a fraction close to 0.58. In the case of a full box (pile height of 6 cm), after this previous preliminary stage of the packing preparation, we remove the grains located above the box level by the horizontal displacement of a metallic bar to level the surface of the pile as in Ref. [19]. Note that this preparation is not equivalent to a pile of this height in a box much higher because the organizations of the superficial grains are quite different: the probability of a grain to be destabilized is biased by the flat denser structure at the top due to this kind of scrapping technique. The other cases are more similar to drum experiments where grains can roll on the bottom surfaces. Following this protocol, we assume that the piles used in our experiments are prepared with the same history of procedure and are thus reproducible.

Similar piles of different heights have been prepared according to the protocol described above and conditioned at different relative humidities RH by considering different times of exposure in different wet atmospheres (see Sec. IV A): at natural conditions to get humidity rates up to 70% (maximum rate reached during the period of the experiment) and in a humidity control chamber to produce higher values. This chamber is a large Plexiglas box (36 cm in width and height and 68 cm in length) to store up to ten piles that can be exposed to an artificial humidity produced by a saturated salt solution mixed with distilled water (RH for NaCl: $\approx$75%, KCl: $\approx$84%, KNO$_3$: $\approx$94%). The relative humidity and the temperature inside the chamber were recorded every 5 min by a USB digital thermohygrometers. The time of exposure of the pile to the wet atmosphere ranges between two days and four weeks, allowing to follow the evolution of the hygroscopic equilibrium through the pile. Except for specific cases where we will mention the conditions, all our experiments were

performed at a temperature between 20 and 22°C and an hygroscopic equilibrium time of one week.

The pile, prepared at a particular humidity, is then placed on the experimental setup on top of a rotating tray. The rotation of this tray, i.e., the tilt angle of the pile, is controlled by an electrical linear actuator which produces a rotating velocity about 0.08°/s, which corresponds to a quasistatic regime given a very small Froude number $Fr = 10^{-8}$. These experiments consist in tilting the pile from the horizontal position up to the maximum angle of the tray, which is about 75°, allowing series of successive avalanches.

The duration of an experiment on a pile is less than 10 min: Taking into account the low velocity of the vapor diffusion process through the grain interstitials, we assume that the quality of the remaining cohesive contacts is not altered. This nonreversibility of the humid contact breakages is one of the key difference with the experiments performed by Gómez *et al.* [39]. Indeed, as the time for a new contact creation is much smaller than the time needed for the creation of a new capillary bridge, if we do not wait enough, no new capillary bridge can occur. But, by opposition, in some of their experiments, they have waited enough to allow these newly created capillary bridges, at least, at the newly created surface of the packing.

B. Principles of the optical measurements

During the experiment, the granular pile is slowly and continuously tilted and the data acquisition consists in recording images of the surface of the pile by the use of two cameras with different points of view of the pile: one oriented normal to the surface, fixed a few centimeters above the pile depending on the focus adjustment, to detect movements of grains at the free surface, and one mounted outside the experimental frame, at a distance of 1 m from the lateral side of the pile and normal to it to measure the angle of the surface of the pile. In the following, they are referred to the surface and lateral cameras, respectively.

The surface camera acquired images every 0.45 s, processed by the use of the well-known free ImageJ software [49]. Image processing of a selected observation area S_0 is based on the difference of two successive images, considering a threshold on the intensity level above the noise level induced by the acquisition conditions. Following the method described in previous works [25,35,37], this allows producing a pixel map of equivalent spheres that have moved from an image to another, defining the surface S of rearranged grains. Low values of the normalized active surface S/S_0 highlight patchworks of isolated slots of closed grains. When S/S_0 tends to 1, a general movement of all the grains located at the surface of the pile is observed, identifying a so-called precursor when no change of the angle of the pile surface is measured. This information can be also assessed by the use of the lateral camera used to follow the angle of the pile surface during the experiment: this camera acquired 30 images per second, with a resolution of 640 by 480 pixels, and a threshold of the gray intensity is applied to generate a white thin band associated to the level of the free surface of the pile. The angle of this band relative to the border of the pile box allows defining the angle

of the pile surface. Interestingly, this indicator can be used to inform also about the rotation speed.

We illustrate these measurements with an experiment performed on a pile of 3 cm in height composed of glass beads of 0.5 mm in diameter placed in a room which relative humidity and temperature are 43% and 26°C (Figs. 1 and 2). The red and blue curves correspond to the results of the analyses based on the surface and lateral cameras, respectively, plotted as a function of the tilt angle in the large range (22–52°) where series of avalanches occurs.

A good agreement and complementarity can be observed between the measurements: The strongest events highlighted by the surface camera are synchronized with the abrupt changes seen on the lateral camera, which correspond to avalanches characterized by a stability and repose angles. The first avalanche appears at the tilt angle 29.5°, preceded in the present case by two precursors and a large number of rearrangements. When the maximum stability angle of the pile θ_A is reached, an avalanche occurs and the surface gets reorganization. At higher angles of the moving plate, series of successive avalanches are detected: we observe a decrease of the stability angle and a nearly constant repose angle. The aim of the present study is studying this behavior by quantifying the stability and repose angles, the angle of appearance of the first precursor and the angle between two successive precursors (interprecursor angle) as a function of relative humidity which effect is expected to depend on the pile structure (height) and the physical properties of the grains (diameter and material).

IV. EFFECT OF HUMIDITY AND PILE HEIGHT

A. Diffusion of humidity inside the pile

In our experiments, we use different grain sizes (D) and materials (glass and polystyrene) and different pile heights (H) which induce differences in the diffusion quality of the RH. In particular, the permeability (k) of the pile, which controls the diffusion of the water vapor inside the pile as a function of the porosity ϕ, tortuosity factor F, and mean pore size according to $k \propto F^{-2} \phi^{3/2} D^2$ for unconsolidated piles [50], is much lower for smaller grains.

For the possible natural relative humidities (RH < 71% in the present study), the grains are initially spread on a flat surface before filling the pile, allowing natural water surface deposition around beads and by consequence a better homogeneity for the adhesive contacts inside the pile for these ambient humidity rates and temperatures. But in the case of higher relative humidity rates (RH > 75%), the packings are prepared initially inside several boxes at ambient humidity and then, stored in a container with a saturated salt solution. Two fans ventilate and homogenize the external artificial water vapor during a given amount of days to diffuse the moisture through the free surface to the inner bulk of the packing (Gómez-Arriaran *et al.* [39]). As a consequence, the diffusion process of the water vapor through all the sample depends on the permeability k of this porous medium and can take some time to reach the full open porous space.

To assess this preliminary analysis, firstly, we have used two sets of three similar piles, composed of 500-μm glass
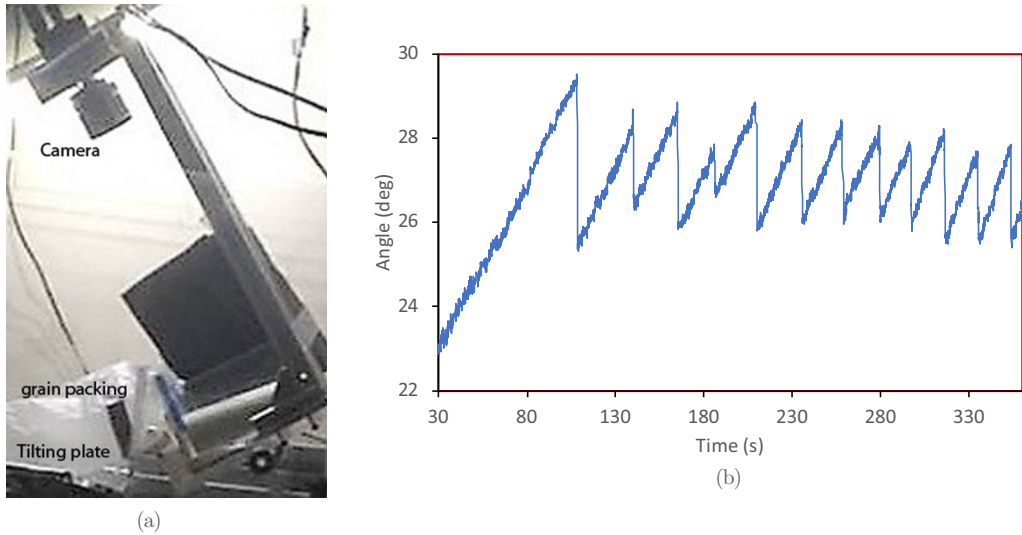
(a)

(b)

FIG. 1. (a) Experimental setup (view from the lateral camera): We can see the top camera moving with the tray, the pile of glass beads inside the small box with a white surface due to the light on top. The linear activator is on the back to permit the slow inclination. (b) Evolution of the surface of the grain packing obtained by an image analysis treatment of the white zone.

beads with a height $H = 4$ cm and stored at RH = 94% and a temperature of $21°C \pm 1°C$ during two days (short storage) and one week (long storage), respectively. For each pile, we performed a tilt experiment by looking at the first maximum stability angle and the four successive ones (Fig. 3). At this relative humidity, the stability angle can be as high as 45°, and we clearly highlight a difference of 8% in degrees between the two storages, with, of course, a lower stability angle for the short storage. In the two cases, the stability angles decrease with the avalanche number and become similar at the end of the experiment. Indeed, as described in the following, after several avalanches inside the box, the full packing of grains have been completely reorganized and all the initial cohesive contacts have lost their initial adhesive properties.

Obviously, the water vapor diffusion inside the pile takes more than two days and the pile cohesion is much stronger for a storage of one week. But suspecting that one week

may be not enough, in particular, for our small grains of $500\,\mu$m which produce a very low permeability, we have then performed two additional sets of experiments on similar piles ($H = 4$ cm) stored, this time, for one and four weeks at a lower humidity of RH = 84% (Fig. 3). In this case, we have measured a relative diminution of the maximum stability angle for the first avalanche of 17% to be compared to the 8% mentioned. But, in complement, for some experiments after the four weeks of humidity impregnation, we have observed that the newly created surface after the first avalanche is no more flat and presents some strong inhomogeneities in volume: few dense humid blocks structures are locally remained. In other terms, for one week, only superficial cake of the packing has cohesive effect due to a partial vapor diffusion through the packing. For four weeks, the vapor diffusion is
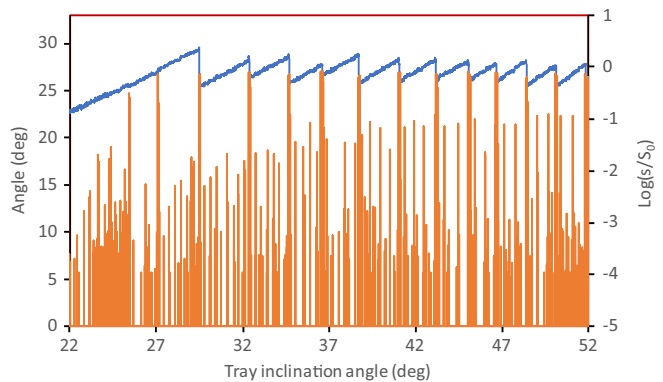

FIG. 2. Synchronization of measurements based on the surface (red curve) and lateral (blue curve) cameras plotted as the tilt angle: S/S_0 close to 1 corresponds to strong events, such as precursors and avalanches, and abrupt changes in the lateral angle, which ranges between 25° and 30°, correspond to avalanches. Large S/S_0 before the first avalanche are defined as precursors (2 in this example).

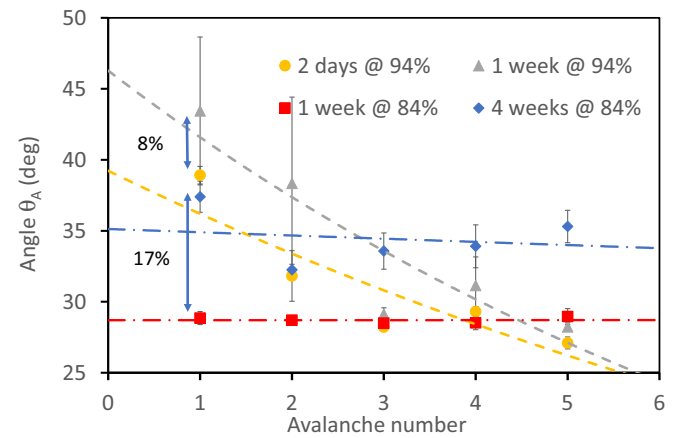FIG. 3. Maximum stability angle measured for two sets of piles stored at RH = 94% and a temperature of $21°C \pm 1°C$ during two days (disk) and one week (triangle) and two sets of piles stored at RH = 84% and a temperature of $21°C \pm 1°C$ during one week (square) and four weeks (diamond). The dashed lines are exponential fits for only eye guides.
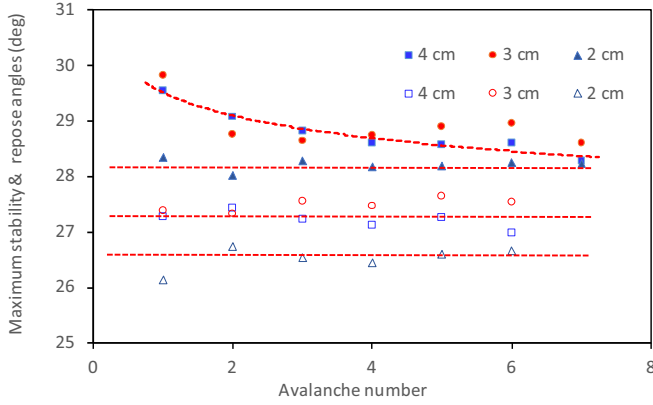
FIG. 4. Influence of the filling height H on the maximum stability θ_A (close symbols) and repose θ_R (open symbols) angles as a function of the avalanche number measured during tilt experiments with glass beads of diameter $D = 500\,\mu$m with a humidity RH = 54% and $T = 21°$C. Each point is a mean value of a minimal of five up to twelve different experiments. The horizontal dashed lines are the mean values of all the points, the dashed line for $H = 4$ cm is only for eyes guidance and it is a best power fit. We observe the same behavior for $H = 5$ or 6 cm than for $H = 4$ cm but with more avalanches going directly outside the box.

going more deeper inside the packing but is not yet perfectly homogeneous for small grains. So neither one week nor four weeks are enough for having homogeneous vapor diffusion inside our packings. From these situations, we can conclude that, in some cases, the avalanches can be controlled mainly by a small superficial cake of strong humid grains on the surface instead of a perfect homogeneous 3D humid packing as expected from this humidity environment. These results have to be compared with the two papers of Gómez-Arriaran *et al.* [39,47] concluding that, for high RH, a minimal duration of two weeks for their packings of $500\,\mu$m glass beads and an height of 6 cm was enough to propagate through all the samples the moisture to generate uniform adhesion forces for all the contacts available inside the packings.

B. Impact on the dynamic of the pile
for different filling heights

All our experiments have been performed with a box of 6 cm in height and the heights H of the piles were set to 2, 3, 4, 5, and 6 cm. For $H = 6$ cm, the box is fully filled and the grains move out of the box since the first avalanche; for a lower H, this requires several avalanches, i.e., the grains start to roll on the bottom of the box wall during the first avalanches. For different heights of a pile composed of grains of diameter $D = 500\,\mu$m with RH = 54%, we performed many tilt independent experiments (between 5 and 12) and measure the average stability angle as a function of the avalanche number (Fig. 4) as already described for the Fig. 3. For $H = 2$ cm, which corresponds to 40 grain diameters, the stability and repose angles are constant, about 28.1° and 26.5°, respectively. We have also observed that $\theta_A(H = 2\,\text{cm})$ is smaller than $\theta_A(H = 3\,\text{cm})$ for the first avalanche and also that $\theta_R(H = 2\,\text{cm})$ is smaller than $\theta_R(H = 3\,\text{cm})$.
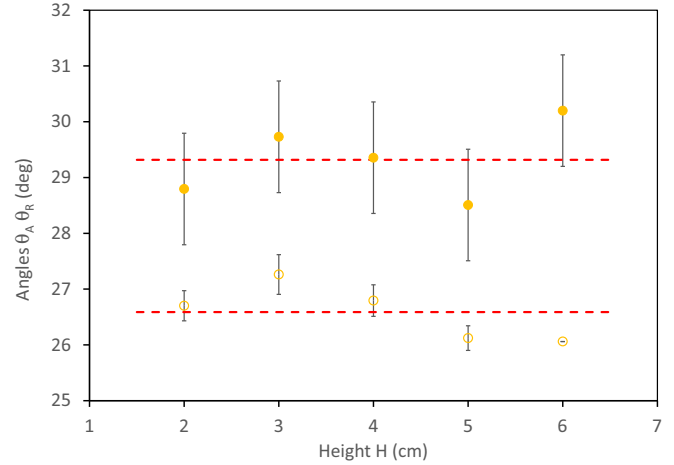

FIG. 5. First maximum stability angles θ_A (closed symbols) and repose angles θ_R (open symbols) for the different filling heights H of the pile measured at all humidity rates lower than 70%. The mean values are obtained in this case from more than 40 experiments at each height H.

These results highlight the influence of the filling rate of the box differently as described in Ref. [24]. Indeed, for $H = 2$ cm, the amount of layers of grains is not enough to allow the conservation of the "bottom wall" effect (i.e., propagation of the ordered structure due to the flat wall) due to a mechanical stability generated by the pressure confinement. By opposition, for higher numbers of layers, the pressure of the grain packings coupled with this "bottom wall" effect can maintain a more stable geometrical structure. In complement, for higher H values, we observe a decreasing trend of the stability angle (θ_A) with the avalanche number, and a nearly stable repose angle (θ_R), in accordance with the results of Gómez-Arriaran *et al.* [39].

In our case, the dynamic behavior of the packing is independent of H when the pile height is above 40 layers ($H \geqslant 3$ cm), which is much more than the 16 layers identified in the experiments of Aguirre *et al.* [16]. The difference may be explained by two geometrical differences. First, in the pile fabrication, we are pulling out a grid to homogenize the pile which creates a lower packing fraction for our piles. Second, the relative size ratios (horizontal surface of the box/grain size) which are, respectively, 17 200 for them (32×26 cm for 2.2 mm sphere diameter) and 28 600 for ours, allow less small rearrangements in their cases and only more global or collective events.

In Fig. 5, we are looking more globally at the different avalanche evolutions. We have focused our analysis on the first avalanche events by considering a large number of experiments (more than 40) performed at different filling heights H with glass beads of diameter $D = 500\,\mu$m under humidity rates lower than 70% (indeed, Fig. 7 confirms that no significant change exist below this value). By reporting the stability and repose angles as a function of H, we showed that a constant trends can be represented for the values of H between 3 and 5 cm as the other cases ($H = 2$ or 6 cm) follow different behaviors and are not taken into account for the trend observation.
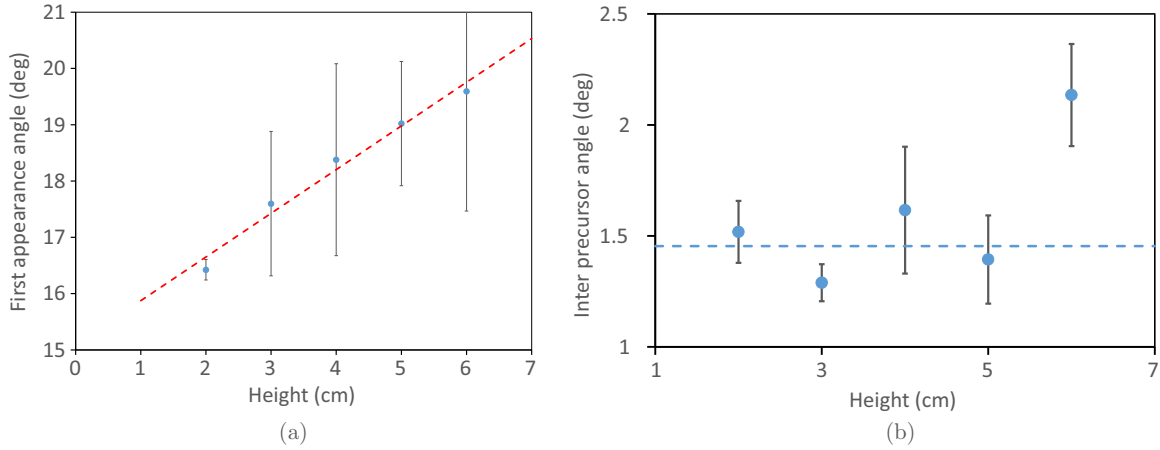
FIG. 6. (a) Appearance angle of the first precursor and (b) interprecursor angle as a function of the pile height, measured for the experiments used in Fig. 5. In (b) we have drawn an horizontal fit as we can assume that the $H = 6$ cm packing has a quite different packing history and cannot be compared directly to the other results.

The difference between θ_A and θ_R is around 2–3°. This general behavior will allow us to assume that we can use all the results obtained with different filling levels for the global analysis of the other parameters evolutions during the series of avalanches.

In addition to the analysis of the stability and repose angles, the dynamic of the pile during tilting is discussed in term of angle of the first precursor (first appearance angle) and increment angles between two successive precursors (inter-precursor angle), both measured as a function of the pile height (Fig. 6).

The results highlight that the higher the filling rate, the higher the first appearance. The interpretation is linked to the fact that a higher internal pressure moves the shearing processes zone to the top of the pile and, by consequence, diminishes the probability of destabilization of the pile under this rupture line. We can also include the "bottom wall" effect as mentioned previously. In Fig. 6(b), we can see that the interprecursor remains constant with H as it will be also observed versus RH as shown later on in the Figs. 8(b) and 13.

For all these analysis on the precursors and avalanches events, we observe that the influence of the height is limited to 2° for θ_A and 4° for the first appearance of precursors which are significantly small compared to the humidity effect that we will describe later on in this paper: the maximum stability angle starts around 27° for RH = 40% to end at 55° for RH = 94% and the first precursor appearance evolution has an amplitude of 20° in the same RH range. So except for specific cases, we will use the possibility of merging all the data to improve the statistical behavior analysis.

C. Contribution of the two effects: Humidity and pile heights

We summarized tilt experiments with different piles of glass beads of diameter $D = 500 \, \mu$m, with heights H from 2 to 6 cm and humidity between 40 and 70% and a temperature around 21°C defined as ambient conditions. For humidities between 75% and 94%, all the samples were stored inside a confined box with the adapted salt for a given RH value during one week. Only for specific test experiments, this duration was modified down to two days or up to four weeks as described
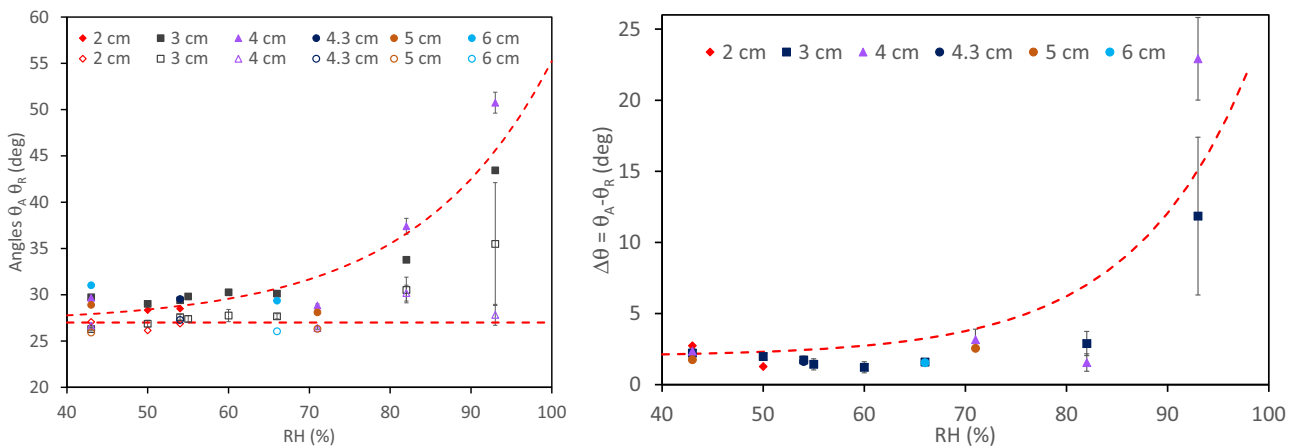

FIG. 7. Evolution of the maximum stability θ_A (closed symbols) and the repose θ_R (open symbols) angles versus the humidity rate for the different available filling heights. The results are shown separately for each set of height H. The dashed lines are only guided lines for a better observation and have an exponential form for θ_A.
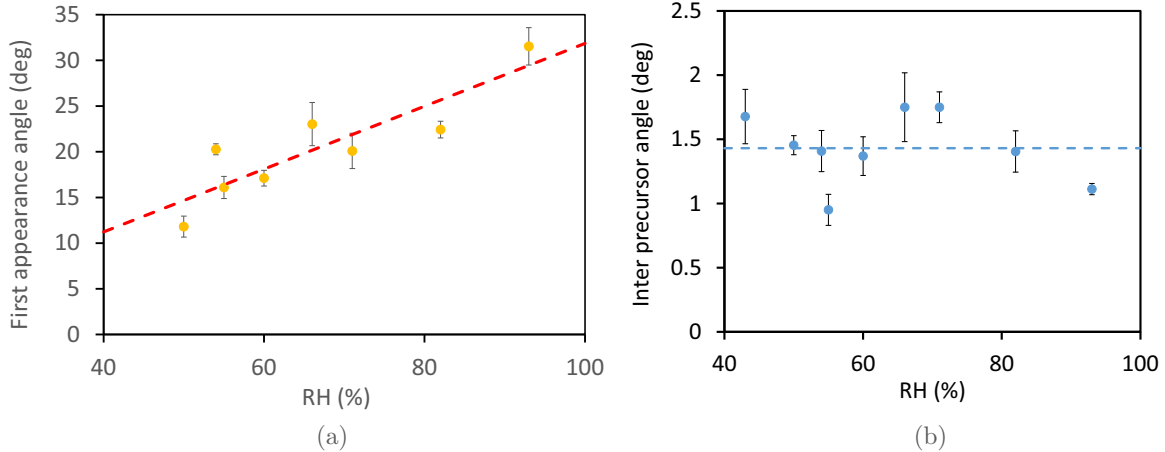
FIG. 8. Evolution of the appearance angle for the first precursor versus the humidity rate RH (a). Evolution of the interprecursor angle versus the humidity rate RH (b).

previously. Then we measured the stability θ_A and repose θ_R angles of the avalanches and the first appearance of precursors and the interprecursor angles.

In accordance with previous discussions and studies [39], the maximum stability angle θ_A increases with the humidity rate, and the repose angle θ_R remains almost constant under natural humidity rates (RH < 70%): with the saturated salt solution and RH > 80% during one week of exposure inside the box, θ_R also increases. The global network of wet contacts between the grains of the pile play a role during the landing of the falling beads as a cushion bed made of linked beads by adhesion forces. Interestingly, the difference between the two angles starts to increase with RH when RH > 90%.

Note that the particular experimental conditions performed with fully filled boxes (pile height H = 6 cm) are very similar to the conditions used in the previous study by Gómez-Arriaran *et al.* [39]: the main differences are the packing fraction which can be smaller in our case due to the grid ejection, the time of exposition to a given RH and the tilting principle. In our sets of experiments, it is regular and continuous during our experiments compared to manually and adaptively very slow. As shown in Fig. 7, the new results are in agreement with the data published by Gómez-Arriaran *et al.* [39] (Fig. 8 on page 29): the global behavior is similar, but lower in magnitude because the very slow tilting approach allows the wet contacts to be remain strongly than in our case. Indeed, as mentioned previously, a cohesive superficial bead layer can be maintained during the very slow tilting process made by Gómez-Arriaran *et al.* [39]: This is not the case here, where the rotating tray is inclined more rapidly and in presence of small vibrations due to the linear activator transmitted to the rest of our setup. In our case, only few broken links between beads can initiate the beginning of the precursor events which end by an avalanche.

As observed for the filling height effect, we can look at the influence of the humidity rate on the first appearance of the precursor and also at mean angle difference between these precursors which are present before the first avalanche (Fig. 8).

We have plotted the values for all the available filling heights used in our experiments (H = 2 to 6 cm) to improve

the statistics of our analyses. We can see an increase of the first precursor appearance with all the humidity rates even in the lower RH part in which no evolution is visible for the maximum stability angle θ_A. This very interesting observation can allow us to qualify the precursor analysis as a more sensible tool for the evolution of the local adhesion force between grains. Indeed, this effect is visible on the surface by the possible grain reorganization during the precursor events. By contrast, we cannot observe any clear evolution of the interprecursor angle value which could be explained as a phenomenon more controlled by the global geometrical organization of the grain packing than by the adhesion force difference with the humidity rates.

V. EFFECT OF HUMIDITY AND GRAIN PHYSICAL PROPERTIES

The effects of the humidity on the dynamic of the pile are more pronounced when we are considering small grains. In the previous sections, we have only described results obtained with beads of diameter D = 500 μm, chosen in accordance to the experiments of Gómez-Arriaran [39] to extend their study on the effects of humidity on the glass bead avalanches to precursor events. In this section, we go further into the analyses by considering smaller and larger grains of different materials: glass beads of diameters 200 μm and 750 μm and polystyrene beads of diameter 140 μm. Note that to assess the effect of the material of the grains on the dynamic behavior of the pile, we will consider glass beads of diameter 200 μm and polystyrene beads of "similar" sizes.

A. Effects of the grain size on the dynamic of the pile

New glass beads have been used for this study, i.e., they have not been used before. For these two new sets of beads, we have measured the adsorption isotherms to quantify the water content of the piles as a function of the RH (Fig. 9). The process is the standard one: After drying 150 mg of glass beads at 80°C with an heating ramp of 5°C per minute inside a controlled chamber during up to 60 min, the piles have been submitted to a RH between 10 and 95%, by steps of 5% at a
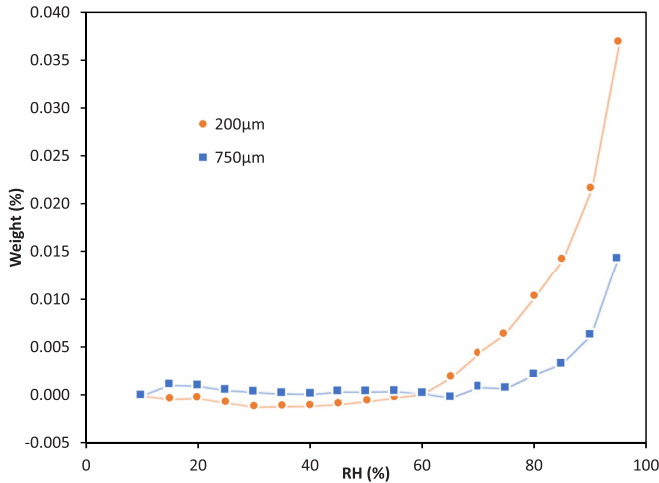
FIG. 9. Influence of the humidity rates on the adsorption isotherms for the two beads diameters used in this study: $200\,\mu$m and $750\,\mu$m.

temperature of 25°C. The equilibrium time for each humidity inside the chamber was defined by a fluctuation smaller than 0.0010% of water content or a maximal time of 5 min.

We observe a large increase of the water content for the 200- and 750-μm glass beads, around 60% for the $200\,\mu$m and 85% for $750\,\mu$m, which can be compared to the location of the slope change point visible for the 500-μm glass beads in Fig. 7. This full behavior evolution is also similar to the observation made by Forny *et al.* [51] for 80-μm beads during the increasing part of their hysteresis isotherms. We can mention that the large hysteresis part obtained during the decrease in their experiments allow us also to confirm the fact that the water content is maintained inside the porous structure even during part of the ambient humidity decrease which occurs as in our case during the experimental process. We were unable to obtain the same data for the 500-μm glass beads and for the polystyrene beads due to the non availability of the equipments. But the close behaviors for the two other sets of glass beads and the general trend of this kind of curves can allow us to assume the same behavior for the 500-μm diameter. These behaviors confirm that we cannot observe significant change for individual contact, or adhesion force at humidity rates lower than 65%.

First, we have looked at smaller beads of $200\,\mu$m. We recover the different evolutions observed for the 500-μm glass beads such as the angles of maximum stability θ_A and repose θ_R versus the avalanche number then these angles versus the humidity rate and finally the first precursor appearance. In the Fig. 10, we have used a pile height of 4 cm for detecting several successive avalanches. In all the other experiments, we have used packings which fully filled the box ($H = 6$ cm). Indeed this filling rate was seen before in this paper as the most easy to manage.

Figure 10 shows the same behavior as the one described in Fig. 4 and in the paper of Gómez-Arriaran [39]. We can notify that the evolution of the angle of repose θ_R is quite similar for both grain diameters which tends to demonstrate that the roughness of the surface structure is not playing a crucial role. Indeed, in our case θ_R (for $D = 200\,\mu$m) is equal
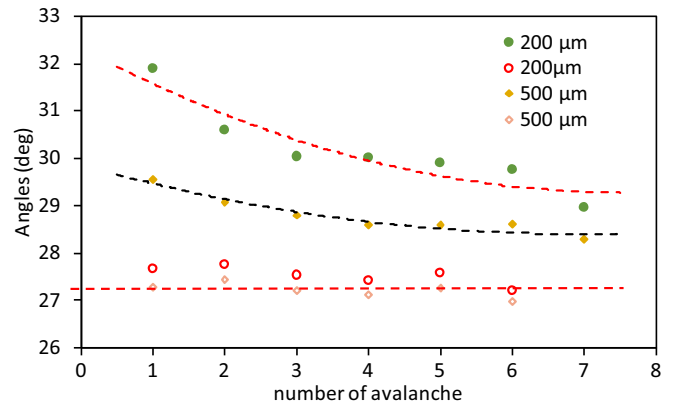

FIG. 10. Evolution of the successive maximum stability θ_A (closed symbols) and the repose θ_R (open symbols) angles behaviors for glass beads of $200\,\mu$m (RH between 43% and 58%) and $500\,\mu$m (RH between 43% and 66%) for an height $H = 4$ cm in both cases. We can recover the classical behavior already seen before (Fig. 4) and visible in Ref. [39]. Each point is a mean value for at least five different runs.

to θ_R (for $D = 500\,\mu$m) for all the humidity rates available (see in Fig. 11).

Figure 11 shows that the behaviors of the maximum stability angles θ_A follow the same profile within this range of humidity rates for the two smaller bead sizes but remain constant for the larger one of $750\,\mu$m. As seen in Fig. 7 and partially in Fig. 10 where RH ranges between 43% and 66%, we can also confirm that the repose angles θ_R are identical for the full range of humidity rates. Figure 11 shows that the maximum stability angle for the 750-μm beads is independent of the humidity rate which is quite different to the results of Gómez-Arriaran [39] made for 1 and 2 mm. This behavior difference is still explained by the "large" inclination speed used in our automatic setup compared to the slow manual motion used by them and also the smaller packing fractions of our samples. Some global mechanical vibrations can also
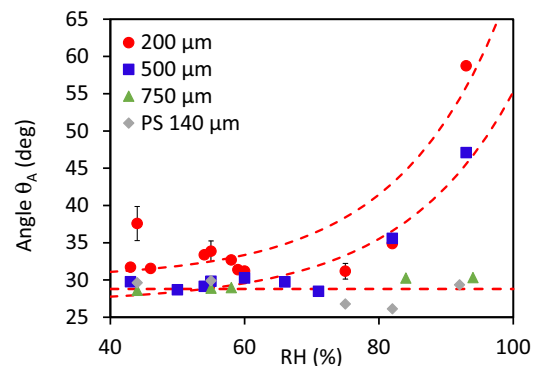

FIG. 11. Evolution of the maximum stability angles θ_A versus the humidity rate for a filling height $H = 6$ cm for glass beads of $200\,\mu$m, $500\,\mu$m, and $750\,\mu$m and polystyrene beads of $140\,\mu$m. The dashed lines correspond to the fits shown in Fig. 7 for the glass beads of $500\,\mu$m and the same equation with different parameters for $200\,\mu$m and a simple horizontal line one for $750\,\mu$m and also for the polystyrene beads of $140\,\mu$m.
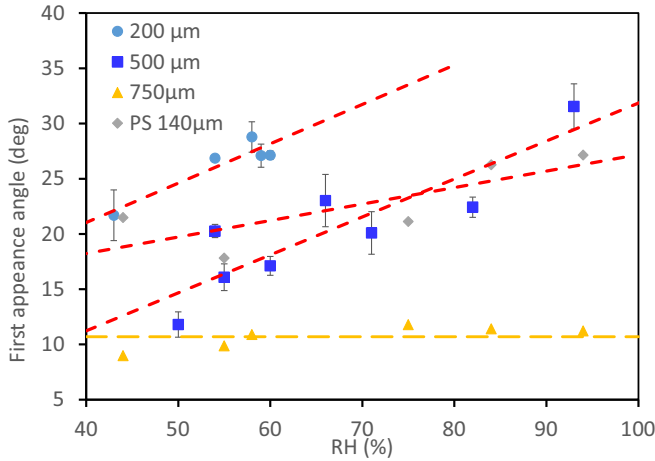
FIG. 12. Evolution of the first precursor angle versus the humidity rate for glass beads of $200\,\mu$m, $500\,\mu$m, and $750\,\mu$m and polystyrene beads of $140\,\mu$m. For the three sets of data, we have plotted the best linear fits and for the $750\,\mu$m we have plotted an horizontal line.

strongly alter the quality of the frictional adhesive contacts especially when the water content rings around the grain contacts are weak compared to the grain weights.

In complement, by using the best linear fit, we can see, in Fig. 12, that the appearance angle of the first precursor is increasing with the humidity rates. This evolution is similar to the one observed for the beads of $500\,\mu$m (Fig. 8). These evolutions of the first precursor appearance in the range of humidity where the maximum stability angle θ_A seems to be quite constant are also dependent of the bead sizes which confirm that this parameter can be a crucial indicator of the "quality" of the contacts. Figure 12 shows that, for the 750-μm glass beads, the first precursor appearance is constant with the humidity rate and much smaller than for the two other smaller glass beads.

In the same manner, in the Fig. 13, as pointed out before, the interprecursor interval remains constant in both cases but with different amplitudes. We have to mention that the measurements for the two smaller bead sizes (200-μm glass
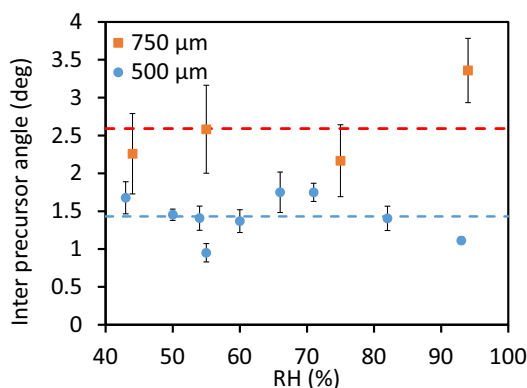

FIG. 13. Evolution of the inter precursor angle versus the humidity rate for a filling height $H = 6\,\text{cm}$ for glass beads of $500\,\mu$m and $750\,\mu$m. The measurements for the two smaller bead sizes were not possible with our setup.

beads and 140-μm polystyrene beads) were not possible with our setup. This amplitude difference is normal if the precursor appearances are mainly dependent of the grain size local structures as suggested in Sec. IV.

B. Effects of the grain material on the dynamic of the pile

Finally, we have extended our studies to the 140-μm polystyrene beads. These beads have a quite different water contact angle $87.4°$ and the critical surface tension is $40\,\text{mN}\,\text{m}^{-1}$ (see Ref. [52]) compared to $22°$ and $70\,\text{mN}\,\text{m}^{-1}$ for glass beads, respectively.

We can see in Fig. 11 that the maximum stability angle of the polystyrene beads is invariant with the evolution of the humidity rate which is consistent with our expectation. Indeed, these polystyrene beads are hydrophobic which means that the water meniscus at the contact point remains very small whatever the humidity rates. As a consequence, cohesion between the polystyrene grains does not increase with humidity: This is clearly highlighted by our experiments, where the linear horizontal fits for the glass beads of $750\,\mu$m and polystyrene beads of $140\,\mu$m are identical. This similarity confirms also the dependency of these maximum stability angles only with the disordered structure of the packing.

Figure 12 shows that the evolution of the first precursor appearance for this new set of beads is not following the same behavior as for the 200-μm glass bead ones. This is a combination of the geometrical effect, i.e., local spatial organization which creates different roughness for the grain stability (comparison with the 200-μm glass beads), the nonwetting contact effect (comparison with the 750-μm glass beads), and finally the different friction coefficient and mechanical properties of the two materials. These facts place the curve between the three other ones and finally confirms the quality of this "stability indicator."

VI. CONCLUSION

By the use of a large set of optical experiments, we characterized the influence of the humidity rates on the dynamic behavior of piles with different heights, size, and properties slowly and continuously inclined up to the avalanche.

Studies reported before have shown the evolution of the successive avalanches which occurred during these tilting processes for both dry and humid cases. In complement, other studies have demonstrated the existence of precursor events such as surface rearrangements of grains before an avalanche: small (few individual grains in movement) and large rearrangements or precursors (number of displaced grains of the order of one surface packing layer) mainly in dry cases. Here, we have confirmed all these previous results, but we have also extended them by demonstrating that these precursors (first appearance and periodicities) are depending to the grain size, grain properties and, more important, of the inner humidity rates all together. Indeed, we have detected an increase of the first precursor appearance for all the range of humidities, grains sizes (except for larger ones) and properties (even for polystyrene beads!) as during the same time, the avalanche events were remaining constant for larger beads and polystyrene ones. In parallel, we have observed that the

interprecursor interval was almost constant for the different grain sizes or humidity ranges studied here. So we can conclude that the precursor observations is a more precise tool for the observation of the grain properties during tilting process.

ACKNOWLEDGMENTS

[1] H. X. Glicken, Rockslide-debris avalanche of May 18, 1980, Mount St. Helens Volcano, Washington, Open-File Report No. 96-677, U.S. Geological Survey, 1996.

[2] E. Bruce Pitman, C. Camil Nichita, A. Patra, A. Bauer, M. Sheridan, and M. Bursik, Computing granular avalanches and landslides, Phys. Fluids **15**, 3638 (2003).

[3] S. Szymczak, M. Bollschweiler, M. Stoffel, and R. Dikau, Debris-flow activity and snow avalanches in a steep watershed of the valais alps (switzerland): Dendrogeomorphic event reconstruction and identification of triggers, Geomorphology **116**, 107 (2010).

[4] C. D. Willett, M. J. Adams, S. A. Johnson, and J. P. K. Seville, Capillary bridges between two spherical bodies, Langmuir **16**, 9396 (2000).

[5] E. Charlaix and M. Ciccotti, Capillary condensation in confined media, in *Handbook of Nanophysics: Principles and Methods*, edited by K. D. Sattler (CRC Press, Boca Raton, FL, 2010).

[6] F. Restagno, L. Bocquet, and E. Charlaix, Where does a cohesive granular heap break? Eur. Phys. J. E **14**, 177 (2004).

[7] L. Bocquet, E. Charlaix, S. Ciliberto, and J. Crassous, Moisture-induced ageing in granular media and the kinetics of capillary condensation, Nature **396**, 735 (1998).

[8] A. J. Liu and S. R. Nagel, The jamming transition and the marginally jammed solid, Annu. Rev. Condens. Matter Phys. **1**, 347 (2010).

[9] L. Oger, A. M. Vidales, R. Uñac, and I. Ippolito, Tilting process with humidity: Dem modeling and comparison with experiments, Granul. Matter **15**, 629 (2013).

[10] Y. Zhang and C. S. Campbell, The interface between fluid-like and solid-like behavior in two-dimensional granular flows, J. Fluid Mech. **237**, 541 (1992).

[11] R. Fischer, P. Gondret, and M. Rabaud, Transition by Intermittency in Granular Matter: From Discontinuous Avalanches to Continuous Flow, Phys. Rev. Lett. **103**, 128002 (2009).

[12] J. Litster and B. Ennis, *The Science and Engineering of Granulation Processes* (Springer, Netherlands, 2004).

[13] M. Bretz, J. B. Cunningham, P. L. Kurczynski, and F. Nori, Imaging of Avalanches in Granular Materials, Phys. Rev. Lett. **69**, 2431 (1992).

[14] N. Nerone, M. A. Aguirre, A. Calvo, I. Ippolito, and D. Bideau, Surface fluctuation in a slowly driven granular system, Physica A **283**, 218 (2000).

[15] N. Nerone and S. Gabbanelli, Surface fluctuations and the inertia effect in sandpiles, Granul. Matter **3**, 117 (2001).

[16] M. A. Aguirre, N. Nerone, A. Calvo, I. Ippolito, and D. Bideau, Influence of the number of layers on the equilibrium of a granular packing, Phys. Rev. E **62**, 738 (2000).

[17] L. Oger, J. P. Troadec, D. Bideau, J. A. Dodds, and M. J. Powell, Properties of disordered sphere packings I. Geometric structure: Statistical model, numerical simulations and experimental results, Powder Technol. **46**, 121 (1986).

[18] V. Yu. Zaitsev, P. Richard, R. Delannay, V. Tournat, and V. E. Gusev, Pre-avalanche structural rearrangements in the bulk of granular medium: Experimental evidence, Europhys. Lett. **83**, 64003 (2008).

[19] S. Kiesgen de Richter, V. Yu Zaitsev, P. Richard, R. Delannay, G. Le Caër, and V. Tournat, Experimental evidence of ageing and slow restoration of the weak-contact configuration in tilted 3d granular packings, J. Stat. Mech. (2010) P11023.

[20] M. Duranteau, V. Tournat, V. Zaitsev, R. Delannay, and P. Richard, Identification of avalanche precursors by acoustic probing in the bulk of tilted granular layers, in *Powders and Grains 2013: Proceedings of the 7th International Conference on Micromechanics of Granular Media, Sydney, Australia*, edited by A. Yu, K. Dong, R. Yang, and S. Luding, AIP Conf. Proc. Vol. 1542 (AIP, Melville, NY, 2013), pp. 650–653.

[21] L. Staron, F. Radjai, and J. P. Vilotte, Granular micro-structure and avalanche precursors, J. Stat. Mech. (2006) P07014.

[22] A. Amon, R. Bertoni, and J. Crassous, Experimental investigation of plastic deformations before granular avalanche, Phys. Rev. E **87**, 012204 (2013).

[23] A. Amon, B. Blanc, and J.-C. Géminard, Avalanche precursors in a frictional model, Phys. Rev. E **96**, 033004 (2017).

[24] M. A. Aguirre, N. Nerone, A. Calvo, I. Ippolito, and D. Bideau, Granular packing: Influence of different parameters on its stability, Granul. Matter **3**, 75 (2001).

[25] S. Kiesgen de Richter, G. Le Caër, and R. Delannay, Dynamics of rearrangements during inclination of granular packings: The avalanche precursor regime, J. Stat. Mech. (2012) P04013.

[26] P. Boltenhagen, Boundary effects on the maximal angle of stability of a granular packing, Eur. Phys. J. B **12**, 75 (1999).

[27] S. Courrech du Pont, P. Gondret, B. Perrin, and M. Rabaud, Wall effects on granular heap stability, Europhys. Lett. **61**, 492 (2003).

[28] W. Bi, R. Delannay, P. Richard, N. Taberlet, and A. Valance, Two- and three-dimensional confined granular chute flows: Experimental and numerical results, J. Phys.: Condens. Matter **17**, S2457 (2005).

[29] J. F. Métayer, Stabilité et propriétés rhéologiques d'empilements granulaires confinés, Ph.D. thesis, Université de Rennes I, 2008.

[30] P. Evesque, D. Fargeix, P. Habib, M. P. Luong, and P. Porion, Gravity and density dependences of sand avalanches, J. Phys. I (France) **2**, 1271 (1992).

[31] N. Gravish and D. I. Goldman, Effect of volume fraction on granular avalanche dynamics, Phys. Rev. E **90**, 032202 (2014).

[32] A. Kabla, G. Debrégeas, J.-M. di Meglio, and T. J Senden, X-ray observation of microfailures in granular piles approaching an avalanche, Europhys. Lett. **71**, 932 (2005).

[33] R. Delannay, M. Duranteau, and V. Tournat, Precursors and triggering mechanisms of granular avalanches, C. R. Phys. **16**, 45 (2015).

[34] A. Jarray, V. Magnanimo, and S. Luding, Wet granular flow control through liquid induced cohesion, Pow. Tech. **341**, 126 (2019).

[35] N. Nerone, M. A. Aguirre, A. Calvo, D. Bideau, and I. Ippolito, Instabilities in slowly driven granular packing, Phys. Rev. E **67**, 011302 (2003).

[36] V. Gibiat, E. Plaza, and P. De Guibert, Acoustic emission before avalanches in granular media, J. Acoust. Soc. Am. **123**, 3142 (2008).

[37] M. Duranteau, Dynamique granulaire à l'approche de l'état critique, Ph.D. thesis, Université Rennes I, 2013.

[38] D. M. Newitt and J. M. Conway-Jones, A contribution to the theory and practice of granulation, Chem. Eng. Res. Design **36a**, 422 (1958).

[39] I. Gómez-Arriaran, I. Ippolito, R. Chertcoff, M. Odriozola-Maritorena, and R. De Schant, Characterization of wet granular avalanches in controlled relative humidity conditions, Powder Technol. **279**, 24 (2015).

[40] J. Crassous, M. Ciccotti, and E. Charlaix, Capillary force between wetted nanometric contacts and its application to atomic force microscopy, Langmuir **27**, 3468 (2011).

[41] H. Rumpf, *The Strength of Granules and Agglomerates* (Interscience Publishers, New York, 1962), pp. 379–418.

[42] S. T. Nase, W. L. Vargas, A. A. Abatan, and J. J. McCarthy, Discrete characterization tools for cohesive granular material, Powder Technol. **116**, 214 (2001).

[43] A. Samadani and A. Kudrolli, Angle of repose and segregation in cohesive granular matter, Phys. Rev. E **64**, 051301 (2001).

[44] S. Nowak, A. Samadani, and A. Kudrolli, Maximum angle of stability of a wet granular pile, Nat. Phys. **1**, 50 (2005).

[45] N. Fraysse, H. Thomé, and L. Petit, Humidity effect on the stability of a sandpile, Eur. Phys. J. B **11**, 615 (1999).

[46] T. G. Mason, A. J. Levine, D. Ertaş, and T. C. Halsey, Critical angle of wet sandpiles, Phys. Rev. E **60**, R5044 (1999).

[47] I. Gómez-Arriaran, I. Ippolito, R. Chertcoff, M. Odriozola-Maritorena, and Y. L. Roht, Dynamic behavior of wet granular media under variable humidity conditions (unpublished).

[48] D. Bideau, E. Guyon, and L. Oger, Granular Media: Effects of Disorder, in *Disorder and Fracture*, edited by J. C. Charmet, S. Roux, and E. Guyon, NATO ASI Series (Series B: Physics) Vol. 204 (Springer, Boston, MA, 1990), pp. 255–268.

[49] https://imagej.nih.gov/ij/index.html.

[50] E. Guyon, L. Oger, and T. J. PLona, Transport properties in sintered porous media composed of two particle sizes, J. Phys. D **20**, 1637 (1987).

[51] L. Forny, I. Pezron, P. Guignon, and L. Kounjer, Peculiar absorption of water by hydrophobized glass beads, Colloids Surf. A **270-271**, 263 (2005).

[52] https://www.accudynetest.com.